J. Ocean Univ. China (Oceanic and Coastal Sea Research)
DOI 10.1007/s11802-009-0015-y
ISSN 1672-5182, 2009 8 (1): 15-22
http://www.ouc.edu.cn/xbywb/
E-mail:xbywb@ouc.edu.cn

Detecting the Relationship Between Summer Rainfall Anomalies in Eastern China and the SSTA in the Global Domain with a New Significance Test Method

LU Chuhan, GUAN Zhaoyong, WANG Panxing*, and DUAN Mingkeng

Department of Atmospheric Science, *Nanjing University of Information Science and Technology*, *Nanjing* 210044, *P. R. China*

(Received November 15, 2007; revised October 23, 2008; accepted November 10, 2008)

Abstract It is suggested that the multiple samples in a correlation map or a set of correlation maps should be examined with significance tests as per the Bernoulli probability model. Therefore, both the contemporaneous and lag correlations of summertime precipitation ***R*** in any one of the three regions of Northern China (NC), the Changjiang-Huaihe River Valley (CHRV), and Southern China (SC) with the ***SSTA*** in the global domain have been tested in the present article, using our significance test method and the method proposed by Livezey and Chen (1983) respectively. Our results demonstrate that the contemporaneous correlations of summer ***R*** in CHRV with the ***SSTA*** are larger than those in NC. Significant correlations of ***SSTA*** with CHRV ***R*** are found to be in some warm SST regions in the tropics, whereas those of ***SSTA*** with NC ***R***, which are opposite in sign as compared to the ***SSTA***-CHRV ***R*** correlations, are found to be in some regions where the mean SSTs are low. In comparison with the patterns of the contemporaneous correlations, the 1 to 12 month lag correlations between NC ***R*** and ***SSTA***, and those between CHRV summer ***R*** and ***SSTA*** show similar patterns, including the magnitudes and signs, and the spatial distributions of the coefficients. However, the summer rainfall in SC is not well correlated with the ***SSTA***, no matter how long the lag interval is. The results derived from the observations have set up a relationship frame connecting the precipitation anomalies in NC, CHRV, and SC with the ***SSTA*** in the global domain, which is critically useful for our understanding and predicting the climate variabilities in different parts of China. Both NC and CHRV summer ***R*** are connected with El Niño events, showing a '– –'pattern in an El Niño year and a '+ +' pattern in the subsequent year.

Key words summer precipitation; eastern China; global sea surface temperature; contemporaneous correlation; time lag correlation; significance test for multiple correlation maps

1 Introduction

Summer drought/flood in Eastern China is the result of the East Asian Summer Monsoon (EASM) precipitation anomaly. Since the 1950s, a great deal of research on the formation mechanism of the precipitation anomaly associated with the EASM has been done from the aspects of atmospheric circulation and external forcing anomaly. It has been recognized that the anomalies of the Western Pacific subtropical high and the middle-latitude westerly circulation are the direct reasons for the summer drought/flood in Eastern China (Ye *et al.*, 1956; Tao and Xu, 1962; Ye *et al.*, 1962; Zhu *et al.*, 1987; Tao *et al.*, 1988; Liao and Zhao, 1990; Chen, 1991; Hu, 1995; Chen and Wu, 1998; Gong *et al*., 2002; Wu *et al.*, 2003; Qin, 2005; and Yang *et al.*, 2007a). The thermal state of the oceans, especially the anomaly of sea surface temperature (***SSTA***) is the most important external forcing factor leading to the anomaly of atmospheric circulation (Lü, 1950; Chen, 1977; Long-Range Weather Forecast Group, 1977; Fu *et al*., 1979; Chen, 1981, 1988; Chen *et al*., 1985; Luo *et al*., 1985; Jin and Luo, 1986; Deng *et al*., 1989; and Yu *et al.*, 2001). The research achievements in this aspect have been summarized by Chen *et al.* (1991) and Ye *et al.* (1996), respectively.

We have noticed that the correlation analysis method (or method whose essence is correlation analysis) is generally used to analyze the relationship between summer drought/flood (or dry/wet) in Eastern China and ***SSTA*** by scholars at home and abroad, and the ocean areas involved have been expanded from the North Pacific at the early stage of the research to the tropical oceans or global oceans at present. However, due to differences in the analysis domain, time period, datasets and evaluation criteria used, the conclusions obtained from the various correlation analyses cannot be directly compared with each other.

This paper focuses on the fundamental problem of the correlation between global ***SSTA*** and the summer ***R*** of three eastern sub-regions (NC, CHRV, and SC) in China, and uses the same data of the same time periods and a unified statistical test scheme in correlation analyses. The

* Corresponding author. Tel: 0086-25-58731519
E-mail: wangpx@nuist.edu.cn

results obtained are beneficial to the understanding of the connection of summer precipitation over Eastern China with global ***SSTA***. And some new insight is gained from a similar analysis of the relationship between summer precipitation over the three eastern sub-regions and El Niño events.

2 Data and Methods and Scheme of Analysis

2.1 Data

Precipitation: the 160 stations under the China Meteorological Administration (CMA), from which the monthly precipitation from 1960–2001 are taken, and the representative stations under the Administration in the three eastern sub-regions are respectively given in Fig.1 and Table 1 (Zhao, 1999).

Sea surface temperature: the global monthly mean SST from the COADS on the $\Delta\lambda\times\Delta\varphi$=2˚×2˚ grid from June 1959–May 2001 from the NOAA-CIRES Climate Diagnostics Center.

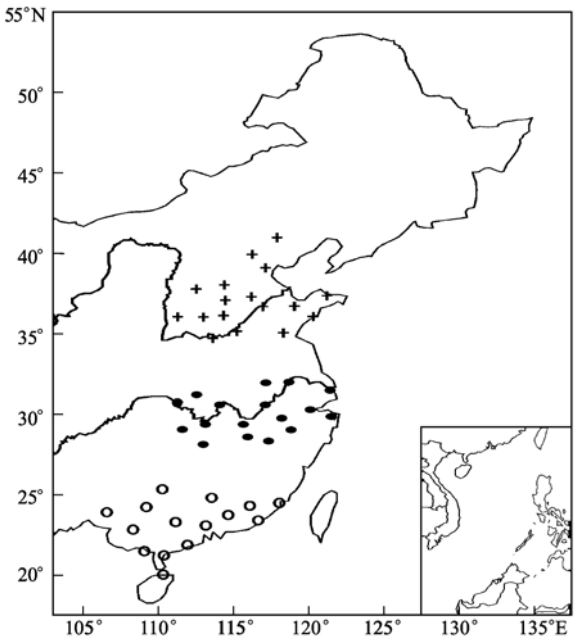

Fig.1 Station distribution in three eastern sub-regions in China. Cross, solid dots and open circles denote NC, CHRV and SC stations respectively.

2.2 Methods of Analysis

In atmospheric science, the basis for the significance test of the results of correlation analysis is the significance test of a correlation coefficient r (assuming the sample size is I). If r passes the significance test at the significance level α ($|r|\geq r_\alpha$), it can be inferred that the two general populations are correlated. Livezey and Chen (1983) presented a significance test method for a set of (J) correlation coefficients (it is generally named a 'correlation coefficient map'). If there are k correlation coefficients (or k points on the map) reaching the significance level α and k is equal to or greater than the critical frequency k_α (*i.e.* $k\geq k_\alpha$), then it can be inferred that the set of correlation coefficients or the 'correlation coefficient map' comes from general correlated populations. Being in accordance with the basic principles of statistical tests, and its result being credible, Livezey's test method is generally accepted.

We consider that the object of current practical correlation analyses is multiple-group experiments or 'multiple correlation coefficient maps'. According to the basic principle of statistical tests, the above two significance tests (one for correlation coefficients, the other for correlation coefficient maps) are not suitable for the test of multiple correlation coefficient maps analysis. Therefore, we propose a significance test method for multiple-group experiments, *i.e.* a significance test method for 'multiple correlation coefficient maps' (Lu *et al.*, 2006), and its basic principles are described as follows.

The test object for 'multiple group experiments' is multiple groups of correlation coefficients or multiple correlation coefficient maps, and its sample may be written as

$$\{\boldsymbol{x}, \boldsymbol{y}_j, j=1,\cdots,J\}_l,\ l=1,\cdots,L, \tag{1}$$

where $\boldsymbol{x}$ denotes the time series of an element; $\boldsymbol{y}_j$ denotes the time series of another element with subscript j, which may indicate a station, a time period or an element; $\{\boldsymbol{x}, \boldsymbol{y}_j\}$ denotes two sample series in one experiment; $\{\boldsymbol{x}, \boldsymbol{y}_j, j=1,\cdots,J\}$ denotes one group experiment consisting of J one-experiments; and $\{\boldsymbol{x}, \boldsymbol{y}_j, j=1,\cdots,J\}_l$, $l=1,\cdots,L$ is a multiple group experiment consisting of L groups of experiments, each group consisting of J one-experiments.

The L groups of correlation coefficients calculated from sample (1) are written as

$$\{r_j, j=1,\cdots,J\}_l,\ l=1,\cdots,L, \tag{2}$$

where r_j is a correlation coefficient, and $\{r_j, j=1,\cdots,J\}_l$ represents a group of correlation coefficients, which is generally a correlation coefficient map. For example, if j denotes a station, it is a geographical distribution map of

Table 1 Representative stations for SC, CHRV, and NC in Eastern China

Sub-region (number of stations)	Representative stations
South China (15)	Xiamen, Meixian, Shantou, Qujiang, Heyuan, Guangzhou, Yangjiang, Zhanjiang, Haikou, Guilin, Liuzhou, Wuzhou, Nanning, Beihai, Baise
CHRV (17)	Nanjing, Hefei, Shanghai, Hangzhou, Anqing, Tunxi, Jiujiang, Hankou, Zhongxiang, Yueyang, Yichang, Changde, Ningbo, Quxian, Guixi, Nanchang, Changsha
North China (17)	Chengde, Beijing, Tianjin, Shijiazhuang, Dezhou, Xingtai, Anyang, Yantai, Qingdao, Weifang, Jinan, Linyi, Heze, Zhengzhou, Changzhi, Taiyuan, Linfen

correlation coefficients, and if j denotes a time period, it is a temporal evolution diagram of correlation coefficients. Expression (2) represents multiple groups of correlation coefficients and it gives multiple correlation coefficient maps.

We recognize that the objects in correlation analyses aiming at short-range climate prediction in the past several years often belong to multiple group experiments (Expression (1)). Therefore, Livezey's test method is not directly applicable to the significance test for Expression (2). However, the problem can be solved if one proceeds as follows.

Based on the Bernoulli probability model, and assuming that each group of samples in Expression (1) comes from independent general populations, at the significance level α the occurrence probability of m groups of $k \geq k_\alpha$ in L groups of correlation coefficients (Expression (2)) is

$$P_L(m) = \binom{L}{m} \alpha^m (1-\alpha)^{L-m}, \tag{3}$$

and the critical value m_α of m can be determined by the expression

$$\sum_{m=0}^{m_\alpha - 1} P_L(m) < 1-\alpha \leq \sum_{m=0}^{m_\alpha} P_L(m). \tag{4}$$

If the assumption of general population independence holds, the occurrence of $m \geq m_\alpha$ maps of $k \geq k_\alpha$ in L maps is a small probability event. Therefore, it can be judged whether the m maps of $k \geq k_\alpha$ in Expression (2) come from correlated general populations or not according as $m \geq m_\alpha$ or $m < m_\alpha$.

It is worth pointing out that, viewing from the multiple group experiments, if $m < m_\alpha$, the samples on the m correlation coefficient maps of $k \geq k_\alpha$ cannot be considered as coming from general correlated populations. Therefore, we cannot use them as the basis for climate analysis and prediction.

2.3 Analysis Scheme

For the purpose of analyzing the connection of sub-region summer $\boldsymbol{R}$ in Eastern China with global ***SSTA***, the following one group and multiple groups of data are selected:

$$\{\boldsymbol{R}, \boldsymbol{SSTA}_j,\ j = 1, \cdots, 868\}, \tag{5}$$

which are for the analysis of contemporaneous correlation, and

$$\{\boldsymbol{R}, \boldsymbol{SSTA}_j(l),\ j = 1, \cdots, 868\}_l,\ l = 1, \cdots, 12, \tag{6}$$

which are for time-lag correlation, where $\boldsymbol{R}$ denotes the regional mean summer (JJA) precipitation series for a sub-region in Eastern China, and its element is

$$R(t_y) = \sum_{s=1}^{n} \sum_{t_m=6}^{8} R(s, t_y, t_m) \Big/ n,$$

where s is the order number of a representative station within the sub-region (Table 1), n is the total number of the representative stations in the sub-region, and $t_y = 1, \cdots, 42$ and $t_m = 6, \cdots, 8$ denote the order numbers of the years and months, respectively. Duan *et al*. (2005) demonstrated the good statistical property of the summer precipitation series of the three eastern sub-regions obtained by following the above analysis scheme. The $\boldsymbol{SSTA}_j$ in Expression (5) is a June-August mean ***SSTA*** series (1960—2001, 42 years in total) covering rectangular longitude-latitude grids ($\Delta\lambda \times \Delta\varphi = 8^\circ \times 4^\circ$, 868 in total) over the Pacific, Atlantic and Indian Oceans, and the $\boldsymbol{SSTA}_j$ in Expression (6) represents the monthly (l) mean ***SSTA*** field series from June of the year $t_y - 1$ to May of the year t_y. Considering the requirements for spatial independence, we preformed Monte Carlo simulation 1000 times for ***SSTA*** field series in $\Delta\lambda \times \Delta\varphi = 2^\circ \times 2^\circ$ (the number of grids was 6801) spatial resolution, and found that the effective numbers of grids for each month were all above 5800, consequently, we reduced the ***SSTA*** series' spatial resolution to $\Delta\lambda \times \Delta\varphi = 8^\circ \times 4^\circ$ (the number of grids was 868), and it can be assumed that they were spatially independent.

For each sub-region in Eastern China, one contemporaneous correlation coefficient map and a set of time-lagged correlation coefficient maps (12 maps in total) can be obtained using sample (5) and sample (6) for contemporaneous/time-lagged correlation analyses, respectively.

3 Simultaneous Correlation Analysis

Computational results show that there is no significant contemporaneous correlation among the summer precipitation series $\boldsymbol{R}$ of the three eastern sub-regions (Table 2). Hereafter, we analyze their contemporaneous correlation with the global June-August ***SSTA***.

Table 2 Contemporaneous correlations of the summer $\boldsymbol{R}$ for NC, CHRV, and SC

Sub-region	r
NC-CHRV	−0.205
NC-SC	0.090
CHRV-SC	−0.067

Notes: The critical correlation coefficient at $\alpha = 0.05$, significance level is $r_{\alpha,l} = 0.304$.

Fig.2 displays the contemporaneous correlation maps of NC and CHRV summer precipitation index with global ***SSTA***, and Table 3 presents the grid number k of $|r| \geq r_{0.05} = 0.304$ for sub-regions NC, CHRV, and SC, respectively. According to Livezey and Chen (1983), at $\alpha = 0.05$, the critical frequency for a correlation coefficient map is $k_{0.05,\,868} = 54$. If $k \geq 54$, it can be judged that the correlation coefficient map comes from general correlated populations. Therefore, it is known from Table 3 that the contemporaneous correlation of summer $\boldsymbol{R}$ of NC and CHRV with ***SSTA***, especially CHRV with it, is significant at the $\alpha = 0.05$ significance level; however, the contemporaneous correlation of SC $\boldsymbol{R}$ with ***SSTA*** is not.

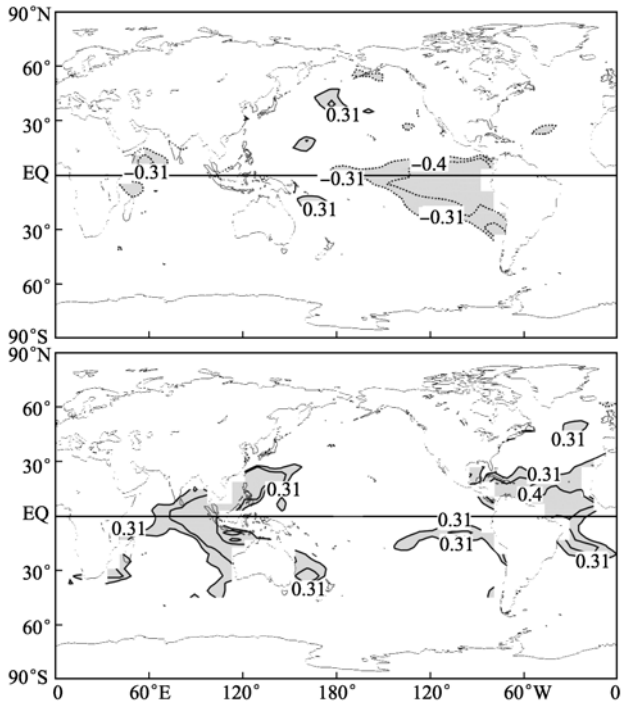

Fig.2 Contemporaneous correlation coefficient maps of sub-region summer precipitation ***R*** and global ***SSTA***. a. NC; b. CHRV. Areas where $|r| \geq r_{0.05}$ are shaded.

Table 3 Grid number k of $|r| \geq r_{0.05}$ on the contemporaneous correlation map of regional summer precipitation and global ***SSTA***

Sub-region	k
NC	**138**
CHRV	**214**
SC	46

Note: Figure in bold denotes $k \geq k_\alpha$, α=0.05.

It follows from Table 3 that the results shown in Figs.2a and b both have passed the significance test for one correlation coefficient map ($k \geq 54$). Therefore, it can be judged that there are significant correlations between the summer precipitation ***R*** in NC and CHRV and global ***SSTA***, and the correlation maps of $k \geq k_\alpha$ come from general correlated populations. The contemporaneous correlation of CHRV ***R*** with global ***SSTA*** is stronger than that of NC ***R***. By contrast, the contemporaneous correlation of SC ***R*** with global ***SSTA*** failed to pass the significance test ($k = 46 < 54$); therefore, the correlation map cannot be regarded as coming from general correlated populations.

Fig.2a shows that the significant correlation areas (hereafter SCAs) for the summer precipitation in NC mainly lie in the central-eastern tropical Pacific and the western tropical Indian Ocean (the Somali current), and these are the climatologically low value (cold water) regions of SST at the same latitude in the season; and negative correlation dominates the relationship between NC ***R*** and global ***SSTA***. By comparison, Fig.2b indicates that the SCAs for summer precipitation in CHRV are mainly distributed in the mid-eastern tropical Indian Ocean, the tropical Northwest Pacific, and the tropical Atlantic, with some smaller SCAs scattered in the East and West Southern Indian Ocean, the Indian Ocean off the coast of South Africa, and the North Atlantic; so the major part of the SCAs lies in the high SST region of the season in the low latitudes (except for the eastern tropical Pacific), and positive correlation dominates the relationship between CHRV ***R*** and global ***SSTA***. It is worth noting that not only the signs of the major SCAs in Figs.2a and b are opposite, but their geographic positions are seldom overlapped (except a smaller area in the eastern tropical Pacific). Fig.3 illustrates this feature and the geographic distribution of the major SCAs of NC and CHRV ***R*** with global ***SSTA***, clearly showing the above distribution characteristics.

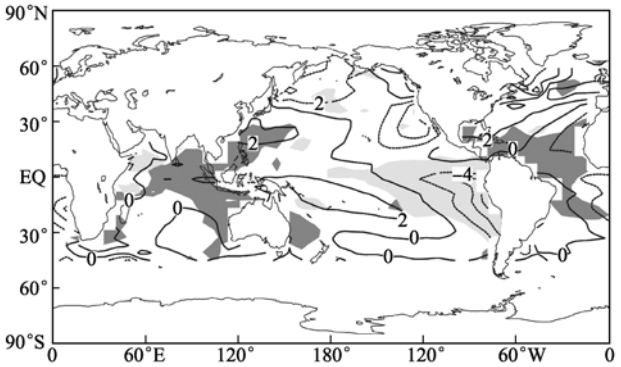

Fig.3 Significant contemporaneous correlation areas of sub-region summer precipitation ***R*** and global ***SSTA***. Dark and light shaded areas denote the SCAs for CHRV and NC, respectively, and solid and dashed lines denote positive and negative deviation contours of SST from the zonal mean (units: ℃; contour interval: 2)

4 Lag Correlation Analysis

For the purpose of forecasting the summer (JJA) precipitation ***R***, the correlation coefficient maps of NC, CHRV, and SC ***R*** with global ***SSTA*** at 1–12 month leads are analyzed. A value of $m_\alpha = 2$ is determined by $\alpha = 0.05$ and $L = 12$.

Table 4 gives the grid number k of $|r_j| \geq r_\alpha$ for each month map, and the m values of the maps of $k \geq k_\alpha$ are 4, 12, and 1 for NC, CHRV and SC, respectively. Therefore,

Table 4 Grid number k of $|r| \geq r_\alpha$ on the correlation maps of NC, CHRV, and SC summer precipitation with the preceding global ***SSTA***

Time		NC	CHRV	SC
Year	Month			
Preceding year	6	17	**199**	27
	7	9	**163**	33
	8	17	**153**	23
	9	17	**123**	16
	10	38	**139**	15
	11	33	**145**	45
	12	44	**156**	**58**
Rainfall year	1	33	**152**	27
	2	**84**	**169**	49
	3	**108**	**216**	39
	4	**72**	**186**	26
	5	**71**	**210**	21

Note: Figure in bold denotes $k \geq k_\alpha$, α=0.05.

from the multiple group experiments, the NC and CHRV summer precipitation are significantly correlated at various month lags with global ***SSTA*** ($m \geq m_\alpha = 2$), and especially, the latter correlation is more typical. However, the SC summer precipitation is not significantly correlated with the preceding global ***SSTA*** ($m < m_\alpha = 2$). Fig.4 displays the correlation map of April global ***SSTA*** with NC summer precipitation ***R***, and Fig.5 shows the correlation maps of monthly global ***SSTA*** at 2-, 5-, 8-, and 11-month leads with CHRV summer precipitation ***R***.

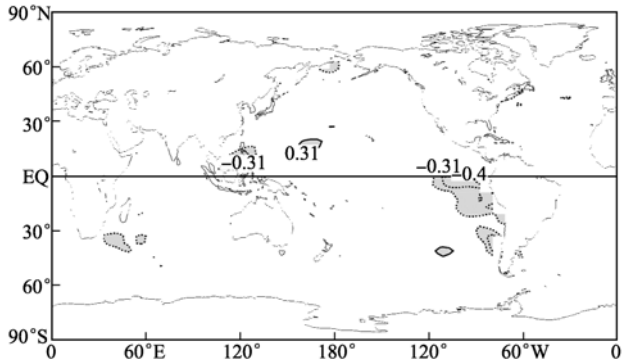

Fig.4 Lag correlation coefficient map of NC summer precipitation ***R*** and April global ***SSTA*** in the same year. Areas where $|r| \geq r_{0.05}$ are shaded.

Comprehensively shown on the correlation maps (Figs.2, 4, and 5) of NC and CHRV summer precipitation ***R*** with global ***SSTA*** are the following regular evolutional rules of the area and position of each of the SCAs. 1) The significant negative correlation area for the lag correlation of NC ***R*** with global ***SSTA*** is located in the eastern equatorial Pacific in spring (Fig.4), and it remains there in summer and spreads over the whole cold water region of the central-eastern Pacific. On each lag correlation map of CHRV ***R*** with global ***SSTA*** (Fig.5) there are SCAs (dominantly positive), whose areas are obviously greater than those in Fig.4; however, the evolution of the areas and positions of the SCAs is complicated. 2) On the lag correlation maps of CHRV ***R*** with global ***SSTA***, the areas and positions of SCAs in the tropical Indian Ocean show annual variation, *i.e.* the areas of SCAs in January of the rainfall year and in July of the previous year are smaller than those in April of the rainfall year and October of the previous year, respectively, while the position (mean latitude) of SCA exhibits an evolution process of north-up-south-down annual oscillation. This phenomenon may be connected with Indian Ocean basin mode (IOBM) (Klein *et al.*, 1999), which affects the intensity Asian southwest monsoon and moisture transport onto east China (Yang *et al.*, 2007b). The evolution of the SCAs in the Pacific Ocean is complicated. In July and October of the previous year (Figs.5a and b), the SCA stably exists in an ocean area near the Philippines and its area seldom changes; in January of the same year (Fig.5c), the main SCA is distributed zonally along the NE direction over the Northwest Pacific, and breaks into two parts near Japan; in April of the same year (Fig.5d), the major SCA is no longer located in the western equatorial Pacific. In the eastern Pacific, the SCA appears from October of the previous year to April of the rainfall year. This is because the ENSO event provides a prolonged impact on the western North Pacific and east Asian climate (Wang *et al.*, 2003), so that it plays an important role in CHRV summer ***R***. Amazingly, the SCAs in the eastern Pacific firstly appear in the northeast extra tropical Pacific in summer of the previous year, and decay as the area of the SCAs increase in the eastern equatorial Pacific, indicating that the extra tropical Pacific is also the key ***SSTA*** anomaly region influencing CHRV summer ***R***.

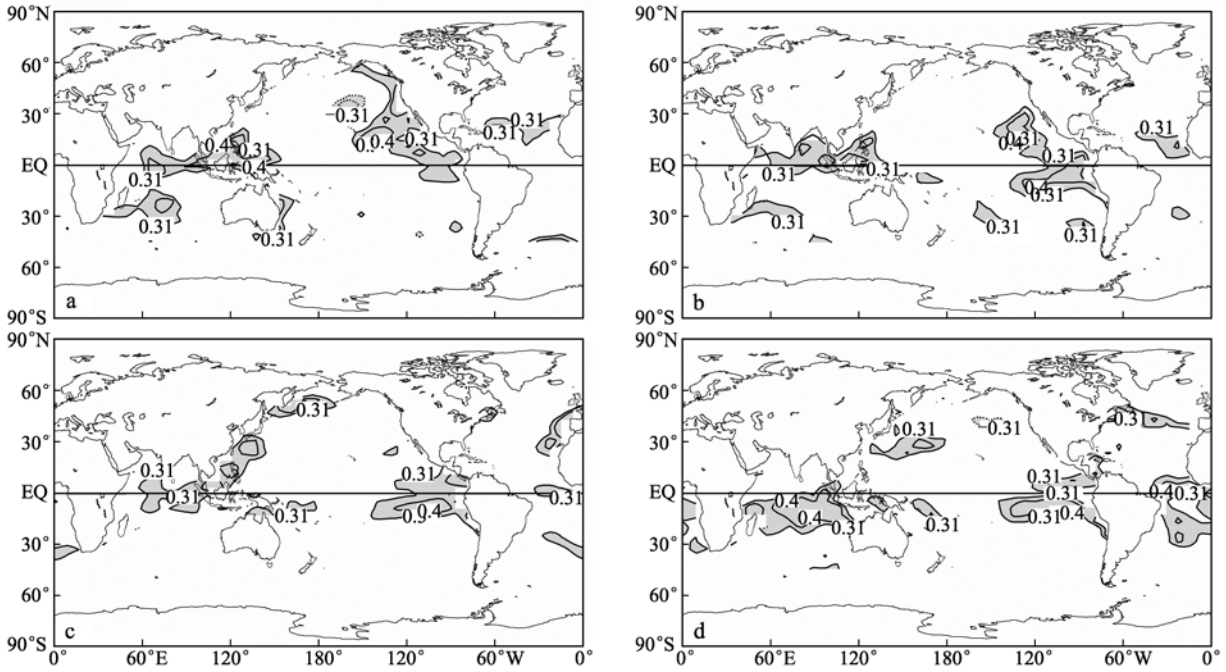

Fig.5 Lag correlation coefficient maps of CHRV summer precipitation ***R*** and the preceding global ***SSTA***. a. July of the previous year; b. October of the previous year; c. January of the same year; d. April of the same year. Areas where $|r| \geq r_{0.05}$ are shaded.

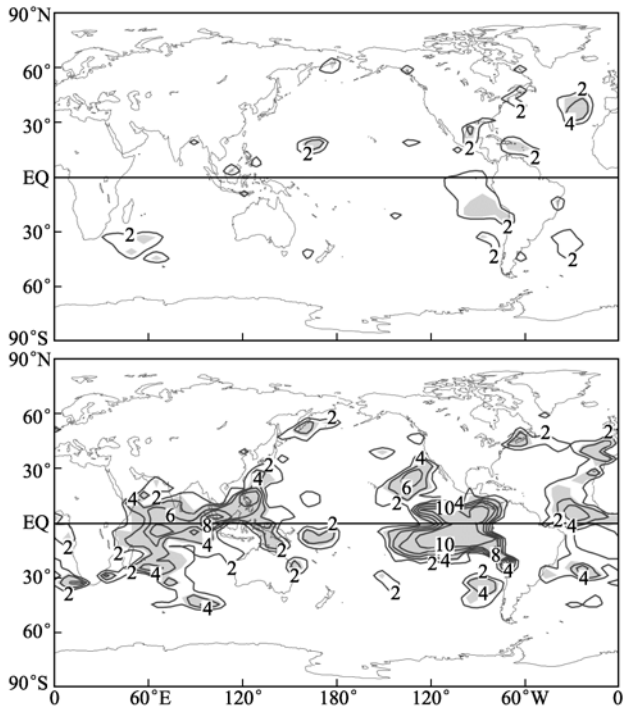

Fig.6 Distributions of month number k_s of the significant lag correlation of NC and CHRV summer precipitation ***R*** with monthly global ***SSTA***. a. NC; b. CHRV. Areas of $k_s \geq 3$ are shaded, and the contour interval is 2.

As a summary of the lag correlation of NC and CHRV ***R*** with global ***SSTA***, Fig.6 gives the grid frequency distribution of the lag correlation coefficients for $|r| \geq r_\alpha$, and shows concentratedly the differences between NC and CHRV in the correlation of global ***SSTA*** in its early stage with the subsequent sub-region summer precipitation ***R***. Obviously, the global ***SSTA*** provides much more information for forecasting CHRV summer ***R*** than for NC; and the SCAs for CHRV are distributed widely over the Pacific, Atlantic and Indian Oceans, while the SCAs for NC are mainly limited to the eastern equatorial Pacific.

5 Correlations Between NC and CHRV Summer Precipitation and El Niño Events

Since the 1980s, a large amount of research work on the relationship between summer precipitation over Eastern China and El Niño events has been done by Chinese researchers, and Ye *et al.* (1996) made a summary that the summer precipitation anomalies over NC, CHRV, and SC in Eastern China exhibit a '– + –'pattern in an El Niño year, and a '+ – +' pattern in the subsequent year. In this study, the time series of the regional mean value [*SST'*] of the monthly SST anomaly over the Nino 3.4 region (5°S–5°N, 120°–170°W） were calculated, and 10 El Niño events (Table 5) from 1960–2001 were determined by using the definition of El Niño ([*SST'*] ≥ 0.5℃ persists for $T \geq 5$ months) given by the Climate Prediction Center (Climate Prediction Center, 2006), and by neglecting the interruption of $t' \leq 2$ months. Correspondingly, 10 El Niño years and the subsequent years were also determined. The statistical results indicate that in an El Niño year, negative anomalies dominate in NC and CHRV summer precipitation, and the occurrence frequencies of negative anomalies are 7/10 and 6/10, respectively; in the next year of the El Niño event, positive anomalies dominate, and the corresponding frequencies are 6/10 and 7/10, respectively (Table 6). Therefore, Ye *et al.*'s (1996) summary is basically correct for NC, but appears to be the contrary for CHRV. The patterns '– –'and '+ +' of NC and CHRV precipitation anomalies slightly dominate in the El Niño year and the next year, respectively, which is obviously different from Ye *et al.*'s (1996) summary. Besides, as El Niño events mostly started at a time later than the end of spring (9/10), it is impossible to predict the summer precipitation anomaly (– –) of NC and CHRV in the El Niño year by monitoring the early stage SST anomaly; however, it is possible to predict the precipitation anomaly (+ +) in the next year by monitoring the SST in the Niño 3.4 region with a certain degree of accuracy.

The formation of the dominant anomaly pattern '– –' or '+ +' for NC and CHRV summer precipitation in the El Niño event year can be interpreted by using the relationship between the contemporaneous SCAs of NC and CHRV summer precipitation ***R*** with global ***SSTA*** in Fig.2, and the key area of the SST anomaly of El Niño events. The SCAs in Fig.2 are mainly distributed in the tropical ocean areas (30°S–30°N). Because the SST anomaly with high absolute values appears in a specific sea region in El Niño events, it has an important effect on the computation of the correlation coefficient in the sea region. According to Wang *et al.*'s (2001) sub-region SVD analyses of the relationship between air-sea interaction over the tropical

Table 5 Time periods of 10 El Niño events from 1960–2001, and the values of index ***R*** for the same and subsequent years

Serial No.	El Niño period	Same year	Subsequent year	Same year ***R***		Subsequent year ***R***	
				NC	CHRV	NC	CHRV
1	1963.7–1964.1	1963	1964	+0.948	–0.657	+0.939	–0.541
2	1965.6–1966.4	1965	1966	–0.511	–0.149	+0.327	–0.755
3	1968.11–1970.1	1968	1969	–1.005	–0.590	–0.153	+1.235
4	1972.5–1973.3	1972	1973	–0.631	–0.709	+0.733	+0.077
5	1976.9–1977.1	1976	1977	+0.437	–0.523	+0.219	+0.359
6	1982.5–1983.6	1982	1983	–0.021	+0.181	–0.961	+0.686
7	1986.8–1988.1	1986	1987	–0.735	–0.186	–0.294	+0.248
8	1991.4–1992.6	1991	1992	–0.476	+0.210	–0.700	–0.236
9	1994.7–1995.3	1994	1995	+0.283	+0.050	+0.361	+0.367
10	1997.5–1998.5	1997	1998	–1.251	+0.245	+0.359	+1.233

oceans and ENSO, the ENSO characteristics are most pronounced in the central-eastern tropical Pacific (175˚E–80˚W), less pronounced in the tropical Indian Ocean (50˚–100˚E), and least pronounced in the western tropical Pacific (120˚–170˚E); They are not evident in the tropical Atlantic Ocean (50˚W–0˚). The reason for a negative ***R***' (precipitation anomaly) for NC and CHRV in the El Niño year can be statistically interpreted as follows: the negative SCA of NC summer ***R*** with global ***SSTA*** in Fig.2a lies in the central-eastern tropical Pacific (the key area of strong ***SSTA*** in ENSO events; see Wang *et al.*, 2001), wherein most summer ***SSTA*** (7/10) in El Niño years are positive, and, therefore, the summer ***R***' for NC in the same year of the El Niño event is negative. The most prominent SCAs of CHRV summer ***R*** with global ***SSTA*** in Fig.2b are mainly distributed in the eastern tropical Indian Ocean, the western Pacific, and the western Atlantic Ocean, indicating that the connection of CHRV summer ***R***' with El Niño events is weaker. The SCAs of CHRV ***R*** with global ***SSTA*** are all positive, while ***SSTA*** in these ocean areas in the same year of El Niño events are generally negative, and, therefore, the possibility that the CHRV summer ***R***' is negative is larger.

Table 6 Frequencies for NC and CHRV summer precipitation anomalies in the same and subsequent years of the 10 El Niño events from 1960–2001

El Niño event	NC		CHRV		Summary	
	+	–	+	–	NC	CHRV
Same year	3	7	4	6	–	–
Subsequent year	6	4	7	3	+	+

6 Conclusions

The contemporaneous and lag correlation coefficient maps of NC, CHRV, and SC summer precipitation ***R*** with global ***SSTA*** have been tested using Livezey's test method for one correlation coefficient map and the test method for a set of correlation coefficient maps presented by Lu *et al*. (2006). The results suggest that 1) NC and CHRV summer ***R*** are significantly/contemporaneously correlated with global ***SSTA***, and the correlation for CHRV is stronger than that for NC. The SCAs are mainly of positive correlation for CHRV, and negative correlation for NC. The SCAs are mainly distributed in the tropical ocean areas isolated or connected to a certain extent with cold/warm water regions. 2) NC and CHRV summer ***R*** are significantly correlated with the global ***SSTA*** 1–12 months before the summer. As is similar to the contemporaneous correlation, the degree of lag correlation of CHRV summer ***R*** with preceding global ***SSTA*** and the areas and distribution range of SCAs are all greater than those for NC, and the correlations for CHRV and NC are mainly positive and negative, respectively. 3) The contemporaneous and lag correlations of SC summer ***R*** with global ***SSTA*** are both not evident. The above analysis results provide a framework of the association of NC, CHRV, and SC summer ***R*** with global ***SSTA***, which is fundamental for studies on NC, CHRV, and SC summer precipitation anomalies in Eastern China and their prediction. 4) The patterns '– –'and '+ +' of NC and CHRV precipitation anomalies slightly dominate in an El Niño year and the subsequent year, respectively.

Acknowledgments

This paper was supported by the project 'the Weather Cause of Formation for Blizzard Hazard in South China' from the Ministry of Science and Technology National Technological Support Project (2008BAC48B02).

References

Chen, J. Y., 1991. *Studies on the Analysis and Long-Range Forecast of Droughts/Floods in China*. Agricultural Press, Beijing, 341pp (in Chinese).

Chen, L. T., 1977. Influence of eastern equatorial Pacific SST anomaly on tropical atmospheric general circulation and rainy-season precipitation in China. *Sci. Atmos. Sin.*, **1**: 1-12 (in Chinese with English abstract).

Chen, L. T., 1981. Interaction of North Pacific subtropical high and eastern equatorial Pacific SST. In: Collected Papers on Medium-Long Range Hydrological and Meteorological Forecasts (II). Changjiang River Valley Planning Office, ed., Wuhan, China, 335-347 (in Chinese).

Chen, L. T., Jin, Z. H., and Luo, S. H., 1985. Variation characteristics of Indian Ocean and South China Sea SSTs and their relations with atmospheric general circulation, *Acta Oceanol. Sin.*, **7**: 103-110 (in Chinese with English abstract).

Chen, L. T., 1988. Zonal anomaly of tropical Indian ocean SST and its influence on the Asian summer monsoon. *Sci. Atmos. Sin.*, **12** (special issue). 142-148 (in Chinese with English abstract).

Chen, L. T., and Wu, R. G., 1998. Relationship between summer rainbelt patterns in the eastern China and 500 hpa circulation anomalies over the Northern Hemisphere. *Sci. Atmos. Sin.*, **22** (6): 849-857 (in Chinese with English abstract).

Chen, L. X., Zhu, Q. G., Luo, H. B., He, J. H., Dong, M., and Feng, Z. Q., 1991. *The East Asian Monsoon*. China Meteorological Press, Beijing, 362pp (in Chinese).

Climate Prediction Center, 2006. Http://www.cpc.ncep.noaa.gov/products/analysis_monitoring/ensostuff/ensoyears.shtml.

Deng, A. J., Tao, S. Y., and Chen, L. T., 1989. Temporal distributive characteristics of sea surface temperature in the Indian Ocean and its relation to the rainy season precipitation in China. *Sci. Atmos. Sin.*, **13**: 393-399 (in Chinese with English abstract).

Duan, M. K., Wang, P. X., and Lin, K. P., 2005. Analyses of the interdecadal and interannual variations of summer precipitation anomalies in eastern China. *J. Nanjing Inst. Meteorol.*, **28** (1): 93-100 (in Chinese with English abstract).

Fu, C. B., Sun, C. X., and Zhang, J. Z., 1979. The atmospheric vertical circulation during anomalous periods of sea surface temperature over equatorial Pacific ocean. *Sci. Atmos. Sin.*, **3** (1): 50-57 (in Chinese with English abstract).

Gong, D. Y., Zhu, J. H., and Wang, S. W., 2002. Significant correlation between summer precipitation over the Changjiang River Basin and preceding Arctic Oscillations. *Chin. Sci. Bull.*, **47** (7): 546-549 (in Chinese with English abstract).

Hu, Z. Z., 1995. Spatial/temporal evolution characters of rainy-season precipitation over the Yellow River Basin. In: Collected Papers for Chinese Academy of Science KY85-10

Project. China Meteorological Press, Beijing (in Chinese).

Jin, Z. H., and Luo, S. H., 1986. On the relationship between rainfall anomaly in middle and lower Yangtze Valley during the Mei-Yu season and the anomaly of sea-surface temperature in South China Sea. *Acta Meteorol. Sin.*, **44** (3): 368-372 (in Chinese).

Klein, S. A., Soden, B. J., and Lau, N.-C., 1999. Remote sea surface temperature variations during ENSO: Evidence for a tropical atmospheric bridge. *J. Clim.*, **12**: 917-932.

Liao, Q. S., and Zhao, Z. G., 1990. Relationship between East Asian blocking pattern and Western Pacific subtropical high and its influence on precipitation over China. In: Collected Papers on Long–Range Weather Forecasts. China Meteorological Press, Beijing, 125-135 (in Chinese).

Livezey, R. E., and Chen, W. Y., 1983. Statistical field significance and its determination by Monte Carlo techniques. *Mon. Wea. Rev.*, **111** (1): 46-59.

Long-Range Weather Forecast Group, Geographic Institute, Chinese Academy of Sciences, 1977. Impact of tropical ocean's SST on the secular variation of the subtropical high. *Chin. Sci. Bull.*, **22**: 313-317 (in Chinese with English abstract).

Lu, C. H., Wang, P. X., Duan, M. K., and Wu, H. B., 2006. Significance testing for a set of correlation coefficient maps and its application (submitted to *J. Nanjing Inst. Meteorol.*).

Luo, S. H., Jin, Z. H., and Chen, L. T., 1985. Analyses on correlation between the sea surface temperatures in the Indian ocean and South China Sea and summer precipitation in the middle and lower reaches of Changjiang River. *Sci. Atmos. Sin.*, **9**: 314-320 (in Chinese with English abstract).

Lü, J., 1950. Sea surface temperature and dry/wet problem. *Acta Meteorol. Sin.*, **21**: 1-16 (in Chinese with English abstract).

Qin, J., 2005. Diagnostic studies on the inter-annual and inter-decadal variability characteristics of the Arctic Oscillation. Master thesis. Nanjing University of Information Science and Technology (in Chinese).

Tao, S. Y., and Xu, S. Y., 1962. Some aspects of the circulation during the periods of the persistent drought and flood in Yangtze and Hwai-Ho Valleys in summer. *Acta Meterol. Sin.*, **32** (1): 1-10 (in Chinese with English abstract).

Tao, S. Y., Zhu, W. M., and Zhao, W., 1988. On the interanuual variation of Mei-yu. *Sci. Atmos. Sin.*, **22** (special issure): 13-21 (in Chinese with English abstract).

Wang, B., Wu, R., and Li, T., 2003 Atmosphere-warm ocean interaction and its impacts on the Asian-Australian monsoon variation. *J. Clim.*, **16**: 1195-1211.

Wang, P. X., He, J. H., Guo, P. W., and Ma, L. P., 2001. Regional differences of temporal-spatial characteristics of air-sea interactions in tropical oceans. *Acta Meterol. Sin.*, **24** (4): 348-362.

Wu, G. X., Chou, J. F., Liu, Y. M., Zhang, Q. Y., and Sun, S. Q., 2003. Review and prospect of the study on the subtropical anticyclone. *Sci. Atmos. Sin.*, **27** (4): 503-517 (in Chinese with English abstract).

Yang, J. L., Li, Q. Y., Xie, S. P., Liu, Z. Y., and Wu, L. X., 2007a. Impact of the Indian Ocean SST basin mode on the Asian summer monsoon. *Geophys. Res. Lett.*, **34**, L02708, doi: 10.1029/2006GL028571.

Yang, X. Y., Wang, P. X., Qin, J., and Lu, C. H., 2007b. Multi-scale teleconnection of North Atlantic and North Pacific SSTs and its relation to the Asian-West Pacific summer monsoon anomaly. *J. Nanjing Inst. Meteorol.*, **30** (2): 194-200 (in Chinese with English abstract).

Ye, D. Z., Huang, R. H., Ding, Y. H., Li, C. Y., Song, Z. S., and Yuan, C. G., 1996. *Dry/Wet Changes in the Changjiang and Huanghe River Valleies and Their Mechanisms*. Shangdong Science and Technology Press, Jinan, 222-257 (in Chinese).

Ye, D. Z., Tao, S. Y., Zhu, B. Z., Yang, J. C., and Chen, L. X., 1962. *Studies on Northern Winter Blocking Patterns*. Science Press, Beijing, 135pp (in Chinese).

Ye, D. Z., Yang, J. C., Gao, Y. X., Xu, M. Y., Xu, S. Y., and Qiu, L., 1956. *Precipitation over the Yellow River Basin*. Science Press, Beijing, 134pp (in Chinese).

Yu, R. C., Zhang, M. H., Yu, Y. Q., and Liu, Y. M., 2001. Summer monsoon rainfalls over mid-eastern China lagged correlated with global SSTs. *Adv. Atmos. Sci.*, **18** (2): 179-196.

Zhao, Z. G., 1999. *Summer Dry/Wet and the Environmental Field in China*. China Meteorological Press, Beijing, 1-16 (in Chinese).

Zhu, W. M., Zhao, W., and Tao, S. Y., 1987. The circulation characteristics of the East Asian monsoon in the typical summer drought/flood year of 1978/1980 over the Changjiang-Huaihe River Valley. In: Collected Papers of Meteorological Scince and Technology- the East Asian Summer Monsoon (II), China Meteorological Press, Beijing, 36-44 (in Chinese).

(Edited by Xie Jun)